Perturbative analytic theory of an ultrahigh-Q toroidal microcavity

Bumki Min, Lan Yang, and Kerry Vahala
Thomas J. Watson Laboratory of Applied Physics, California Institute of Technology, Pasadena, California 91125, USA
(Received 13 February 2007; published 20 July 2007)

A perturbation theoretic approach is proposed as an efficient characterization tool for a tapered fiber coupled ultrahigh-quality factor (Q) toroidal microcavity with a small inverse aspect ratio. The Helmholtz equation with an assumption of quasi-TE/TM modes in local toroidal coordinates is solved via a power series expansion in terms of the inverse aspect ratio and the expanded eigenmode solutions are further manipulated iteratively to generate various characteristic metrics of the ultrahigh-Q toroidal microcavity coupled to a tapered fiber waveguide. Resonance wavelengths, free spectral ranges, cavity mode volumes, phase-matching conditions, and radiative Q factors are derived along with a mode characterization given by a characteristic equation. Calculated results are in excellent agreement with full vectorial finite-element simulations. The results are useful as a shortcut to avoid full numerical simulation, and also render intuitive insight into the modal properties of toroidal microcavities.

DOI: 10.1103/PhysRevA.76.013823 PACS number(s): 42.60.Da, 42.81.Qb, 45.10.Hj, 47.11.Fg

INTRODUCTION

Ultrahigh-quality factor (Q factor) silica toroidal microcavity resonators have been studied intensively for the last several years [1]. These chip-based microcavities share certain features with microsphere resonators [2]. In particular, their fabrication relies on surface tension induced smoothing of a silica-based whispering gallery resonator to attain ultrahigh-Q performance. Significantly, however, toroidal structures are silicon-chip-based devices and hence wafer-based process tools can be leveraged in their creation, electrical control can be conveniently added [3], and there is the possibility of integration with other devices as well as the addition of MEMs-based control features. Also, the modal spectrum of the toroidal structures is vastly simplified in comparison to spherical devices owing to the exclusion of numerous transverse modes by the toroidal confinement. In terms of applications, the toroidal geometry, in addition to providing an excellent platform for the creation of Raman [4] and rare-earth-based lasers [5,6], offers a unique feature, the ability to phase match a third-order parametric process by control of toroid aspect ratio [7,8]. Also, their high Q factor, small mode volume, and ability to be taper coupled with high efficiency make them interesting candidates for the study of cavity QED related phenomena [9,10]. Recently, they have also been used to sense heavy water at record-low concentration levels [11] and the ability to attain Q factors in excess of 100 million in an aqueous bath [12] makes them likely candidates for biosensing applications.

Despite their important physical properties and applications, modeling the modal properties of toroidal resonators is far more challenging than in spherical resonators. The cavity mode field of the toroidal microcavity has not been solved in closed form. Therefore, the useful metrics of the toroidal microcavity such as cavity mode volumes, radiative (whispering-gallery) Q factors, phase-matching conditions, resonance wavelengths, and free spectral ranges (FSR) could not be explicitly calculated, and it has been necessary to resort to numerical simulation [9]. The complication of obtaining approximate solutions arises from the inseparability of a scalar wave equation in local toroidal coordinates and the corresponding lack of knowledge for the solutions of these two-dimensional problems. In this paper, we show that the difficulty of obtaining analytic solutions can be circumvented, and an approximate solution can be obtained by applying a perturbation method using a proper expansion parameter for a "fiberlike" (small inverse aspect ratio) toroidal geometry. An iterative perturbation expansion method will be applied to calculate the cavity mode field inside and near the periphery of a toroidal microcavity with a small inverse aspect ratio (only the bound mode approximation will be considered in this article by modeling the exponentially decaying field outside the toroidal microcavity boundary). The approximate cavity mode field in a small inverse aspect ratio toroidal microcavity can be obtained, in principle, by transforming the Helmholtz equation in a Cartesian coordinate system into a scalar wave equation in the local toroidal coordinates [13]. As a result of this transformation, solutions of the transformed wave equation become analytically tractable with the perturbation expansion to a desired order (at the expense of complexity in the solution derived). With the approximate cavity mode field in hand, other useful characteristics are easily obtained. These include the modal volume, resonant wavelength, mode index, and radiation Q factor. The range of applicability of the perturbation approach will also be investigated by comparing the predicted results with those obtained by using a full-vectorial finite element method (FEM) solver.

PROBLEM FORMULATION

A local toroidal coordinate system (r,ϕ,θ) that is intuitively suitable for electromagnetic problems with a toroidal geometry will be used throughout the rest of this paper. Figure 1 shows the local toroidal coordinate system with a rendering of the toroidal microcavity structure ($D=2R$: major diameter, $d=2a$: minor diameter, and $D_p=2R_p$: principal diameter). The inverse aspect ratio δ, defined as the ratio between minor and major diameter a/R, will play an important role in the expansion of the cavity mode field and the subse-

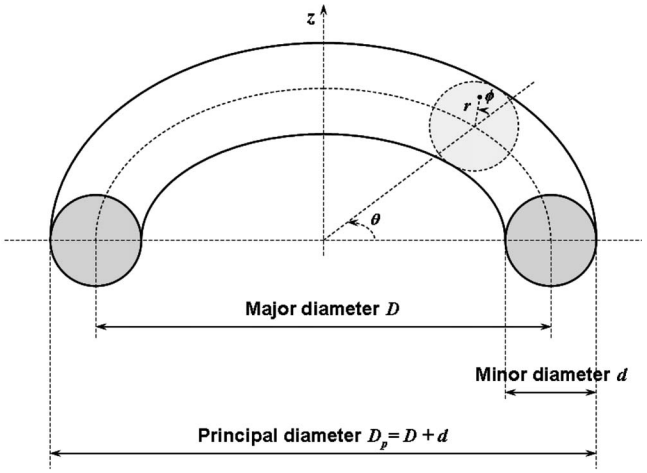

FIG. 1. A local toroidal coordinate system along with a corresponding boundary of the toroidal microcavity. The definitions of principal ($D_p=2R_p$), major ($D=2R$), and minor diameter ($d=2a$) are illustrated along with an axis of rotation in the z direction.

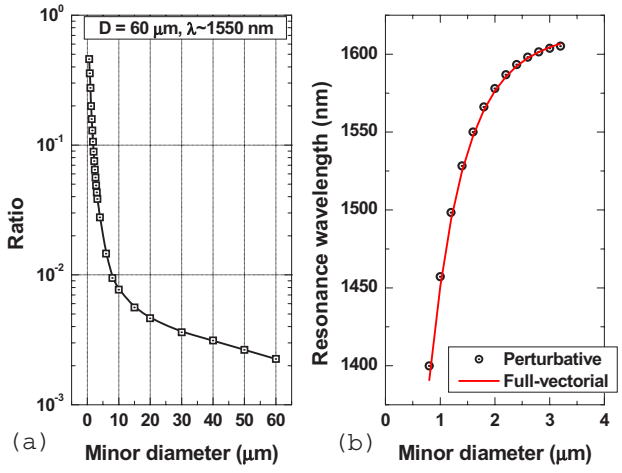

FIG. 2. (Color online) (a) The ratio of the squared nontransverse to transverse electric fields for a fundamental quasi-TE mode (major diameter of the toroidal microcavity is 60 μm and the resonance wavelength is chosen to be around 1550 nm). (b) Resonance wavelength prediction by the perturbative analytic method and the full vectorial model.

quent estimation of various cavity characteristics.

The cavity mode fields in the expansion are treated as quasi-TE or quasi-TM modes. However, fiberlike modes include hybrid solutions, and toroid solutions, in general, are known to include nontransverse components. Therefore, the assumptions of a pure transverse field will need to be investigated. For this purpose, a full-vectorial eigenmode solver is developed for an axially symmetric optical resonator using a commercially available finite element tool. This solver gives the exact eigenmodes (with all six field components) with corresponding eigenfrequencies. By implementing perfectly matched layer (PML) to the arbitrary computational boundary [14], complex eigenfrequencies are obtained and the radiative Q factors are calculated based on these eigenfrequencies. Figure 2(a) shows the relative ratio between the squared nontransverse and transverse electric fields ($|E_\theta|^2/|E_t|^2$) as a function of minor diameter of the toroidal microcavity for a fundamental quasi-TE mode (quasi-TE modes are referred to those modes of which dominant electric field is in the ϕ direction and quasi-TM modes are similarly defined). As can be seen in Fig. 2(a) and, as expected, the toroidal modes are, strictly speaking, hybrid modes. However, the nontransverse electric field remains relatively small until the size of minor diameter approaches the wavelength scale. As a further comparison test of the impact on the calculation of these nontransverse components, the resonance prediction of the full-vectorial calculation and the perturbative analytic model is plotted in Fig. 2(b). The predictions are qualitatively (quantitatively) in agreement in the range of minor diameter studied in this paper regardless of the presence of nontransverse electric field.

In the following sections, the quasi-TE/TM mode approximation will be considered by solving one scalar wave equation perturbatively for the toroidal microcavity with small inverse aspect ratio. Tests of these solutions will be performed by comparing predictions with those of a full-vectorial numerical calculation. Although the derived scalar wave equation is not separable in the transverse plane of propagation due to the coupling term induced by the geometrical perturbation from straight waveguide geometry, the perturbation expansion method can be utilized to give approximate analytic solutions for the transverse fields. The problem of solving the cavity mode field of the toroidal microcavity is very similar to the problem of bent optical fibers. Lamouroux *et al.* solved Maxwell's equation without assuming a weak guidance approximation (which is required for decoupling mode calculation with polarization properties) and obtained a general solution of toroidally bent fibers with all six field components up to the first order [15]. However, the applicability of those solutions to the characterization of the toroidal microcavity is inherently limited due to its complexity in the derived formula.

Since the nontransverse field components can be assumed to be relatively small compared to the transverse field components for the small inverse aspect ratio except for a very small inverse aspect ratio, the scalar wave equation for the transverse field will be used in subsequent evaluations. Then, as has been derived previously for the evaluation of the mode field in the bent optical fibers, the scalar Helmholtz equation can be reduced to the following simple wave equation in transverse local toroidal coordinates after separating the $(1+r/a\cos\phi)^{-1/2}e^{-jm\theta}$ factor (the round-trip phase shift should be multiples of 2π):

$$\left\{\frac{\partial^2}{\partial r^2}+\frac{1}{r}\frac{\partial}{\partial r}+\frac{1}{r^2}\frac{\partial^2}{\partial\phi^2}+k^2n^2\right\}\Psi(r,\phi) + \left(1+\delta\frac{r}{a}\cos\phi\right)^{-2}\left(\frac{1}{4R^2}-\beta^2\right)\Psi(r,\phi)=0, \quad (1)$$

where r and ϕ are the local toroidal coordinates in the transversal plane, k is the wave vector ($k=\omega\sqrt{\mu\varepsilon_0}$) in the free space, n is the refractive index ($=n_0$ for surrounding material), and β is the intrinsic propagation constant defined with

respect to the major radius R (it will be shown later that this intrinsic propagation constant β should be updated to a modified propagation constant β_e by an iterative procedure in order to improve the accuracy of the modeling). This scalar wave equation can be solved to an arbitrary order of δ with an assumption of the quasi-TE/TM mode without separating the wave function into two transverse components. When solving this equation, three integer mode numbers (q,l,m) are naturally introduced to characterize the cavity mode fields. The radial and polar mode numbers q and l determine the type of transverse mode field patterns, and the azimuthal mode number m accounts for azimuthal variations of the cavity mode field. This definition of the mode numbers looks similar to that of the microsphere resonators but has a slightly different meaning and should be distinguished from the mode numbers (q,l,m) for the microsphere resonators [16]. While the fundamental mode of the microsphere resonator is characterized by the condition $q=1$, $l=m$, the fundamental mode $(q=0,\ l=0)$ of the toroidal microcavity resonator is decoupled in terms of polar and azimuthal mode numbers. The transverse electric (magnetic) field can be obtained after solving the wave equation (1) using the perturbation expansion and transforming the wave function according to the formulas as follows:

$$E_z \approx E_\phi = N\left(1+\delta\frac{r}{a}\cos\phi\right)^{-1/2}\Psi_E(r,\phi)e^{-jm\theta}$$

$$\text{(for quasi-TE modes)}, \tag{2}$$

$$H_z \approx H_\phi = N\left(1+\delta\frac{r}{a}\cos\phi\right)^{-1/2}\Psi_H(r,\phi)e^{-jm\theta}$$

$$\text{(for quasi-TM modes)}, \tag{3}$$

where N is a normalization constant obtained from the condition of unit power flow. Quasi-TE modes are defined by $\vec{E}=\hat{z}E_z\approx\hat{\phi}E_\phi$, $E_r\approx 0$, $E_\theta\approx 0$ and quasi-TM modes are defined similarly as $\vec{H}=\hat{z}H_z\approx\hat{\phi}H_\phi$, $H_r\approx 0$, $H_\theta\approx 0$ [17]. As stated before, the mode field cannot be separated in the coordinates (r,ϕ) which is different from the case of microsphere resonators. The intrinsic propagation constant β is defined as

$$\beta=\frac{m}{R}=\frac{m}{R_p-a}. \tag{4}$$

(Note that the major radius R is used in defining the intrinsic propagation constant β, while for a spherical microcavity, the sphere radius R_s, which corresponds to the principal radius R_p of the toroidal microcavity, is used. This discrepancy will be resolved with the definition of the modified propagation constant β_e in the following sections.) Similar to the case of microsphere resonators, this propagation constant can be thought of as the wave vector in the net direction of propagation. However, for a more precise characterization of the cavity modes, this should be updated to a modified propagation constant β_e, as will be made clear later in this paper. The objective of the following section is to derive the cavity mode field in terms of the expansion parameter and to show the actual cavity field modes as the mode number changes [18].

PROPERTIES OF TOROIDAL MICROCAVITY RESONATORS

Using the scalar wave equation expressed in local toroidal coordinates as introduced in the previous section, a perturbational approach similar to the one given in [13], i.e., a power-series expansion can now be applied to provide approximate analytic solutions to the mode field in the toroidal microcavity [19].

Cavity mode field in toroidal microcavity resonators

The intrinsic propagation constant β is quantized to sets of discrete values (given by azimuthal mode number m) and the spacing between adjacent β's is determined by the major diameter of the toroid. If the inverse aspect ratio δ is very small $(\delta=a/R<0.1)$, the error made by approximating the cavity mode field patterns using the second-order expansion for a wave function will be quite small in subsequent characterization. (To increase the accuracy of the results and to use a wider range of minor diameters, the cavity mode field can be expanded further to include higher-order terms.) Making use of the perturbation expansion, we set the wave function in the perturbative form as follows:

$$\Psi=\sum_i \delta^i\Psi^{(i)}. \tag{5}$$

Truncating the wave function expansion up to the second order and inserting it into Eq. (2), the electric field can be expressed as

$$\vec{E}\approx\hat{\phi}E_\phi\approx\hat{\phi}N\left(1+\delta\frac{r}{a}\cos\phi\right)^{-1/2}[\Psi^{(0)}(r,\phi)+\delta\Psi^{(1)}(r,\phi)+\delta^2\Psi^{(2)}(r,\phi)]e^{-j\beta R\theta}, \tag{6}$$

where N is the (power) normalization constant that can be obtained by the volume integral of the squared electric field divided by effective equatorial path length $2\pi R_e$. This power normalization is chosen to study the coupling of a toroidal microcavity with a tapered fiber waveguide in a subsequent section. It will also be used in the estimation of radiative loss using the volume current method. Finally, without any loss of generality, only the quasi-TE mode will be considered in this section to illustrate the computation. The method can be applied to quasi-TM modes in the same way. The scalar wave equation for each order of the expansion is given by

$$D\Psi^{(0)}(r,\phi)=0, \tag{7}$$

$$D\Psi^{(1)}(r,\phi)=-2\beta^2\left(\frac{r}{a}\right)\cos\phi\Psi^{(0)}(r,\phi), \tag{8}$$

$$D\Psi^{(2)}(r,\phi) = -2\beta^2\left(\frac{r}{a}\right)\cos\phi\Psi^{(1)}(r,\phi) + \left[3\beta^2\left(\frac{r}{a}\right)^2\cos^2\phi - \frac{1}{4a^2}\right]\Psi^{(0)}(r,\phi), \tag{9}$$

where the differential operator D is given by

$$D \equiv \left[\frac{\partial^2}{\partial r^2} + \frac{1}{r}\frac{\partial}{\partial r} + \frac{1}{r^2}\frac{\partial^2}{\partial\phi^2} + (k^2n^2 - \beta^2)\right]. \tag{10}$$

After solving the wave equations of each order, the electric fields inside (outside) the transverse toroidal plane can be obtained by substituting the following wave functions into Eq. (6) for the mode number $(q,l,m)=(q,0,m)$:

$$\Psi_{in}^{(0)}(\xi,\phi) = \frac{J_0(u\xi)}{J_0(u)} \quad (\xi \le 1), \tag{11}$$

$$\Psi_{out}^{(0)}(\xi,\phi) = \frac{K_0(u\xi)}{K_0(u)} \quad (\xi \ge 1), \tag{12}$$

$$\Psi_{in}^{(1)}(\xi,\phi) = 2(\beta a)^2 u\xi^2\frac{J_1(u\xi)}{J_0(u)}\left\{\frac{A_0}{\xi^2} - \frac{1}{4u^2}\right\}\cos\phi \quad (\xi \le 1), \tag{13}$$

$$\Psi_{out}^{(1)}(\xi,\phi) = 2(\beta a)^2 w\xi^2\frac{K_1(w\xi)}{K_0(w)}\left\{\frac{B_0}{\xi^2} + \frac{1}{4w^2}\right\}\cos\phi, \quad (\xi \ge 1) \tag{14}$$

$$\begin{aligned}\Psi_{in}^{(2)}(\xi,\phi) = {} & \frac{1}{8u}\frac{J_0(u\xi)}{J_0(u)} + \frac{J_1(u\xi)}{J_0(u)}\left\{-\frac{\xi}{8u} + (\beta a)^2\frac{\xi^3}{4u}\right. \\ & \left. + (\beta a)^2\frac{\xi}{4u}\left[\xi^2 + 4A_0(\beta a)^2\right]\cos 2\phi\right\} \\ & + \frac{J_2(u\xi)}{J_0(u)}\left\{C_0 - \frac{(\beta a)^2\xi^2}{4u^2} - \frac{A_0(\beta a)^4\xi^2}{2} + \frac{(\beta a)^4\xi^4}{16u^2}\right. \\ & \left. + \left[D_0 - \frac{A_0(\beta a)^4\xi^2}{2} + \frac{(\beta a)^4\xi^4}{16u^2}\right]\cos 2\phi\right\} \\ & - \frac{(\beta a)^4\xi^3}{24u^3}\frac{J_3(u\xi)}{J_0(u)} \quad (\xi \le 1),\end{aligned} \tag{15}$$

$$\begin{aligned}\Psi_{out}^{(2)}(\xi,\phi) = {} & \frac{1}{8w}\frac{K_0(w\xi)}{K_0(w)} + \frac{K_1(w\xi)}{K_0(w)}\left\{\frac{\xi}{8w} - (\beta a)^2\frac{\xi^3}{4w}\right. \\ & \left. - (\beta a)^2\frac{\xi}{4w}\left[\xi^2 + 4B_0(\beta a)^2\right]\cos 2\phi\right\} \\ & + \frac{K_2(w\xi)}{K_0(w)}\left\{E_0 - \frac{(\beta a)^2\xi^2}{4w^2} + \frac{B_0(\beta a)^4\xi^2}{2} + \frac{(\beta a)^4\xi^4}{16w^2}\right. \\ & \left. + \left[F_0 + \frac{B_0(\beta a)^4\xi^2}{2} + \frac{(\beta a)^4\xi^4}{16w^2}\right]\cos 2\phi\right\} \\ & + \frac{(\beta a)^4\xi^3}{24w^3}\frac{K_3(w\xi)}{K_0(w)} \quad (\xi \ge 1),\end{aligned} \tag{16}$$

where $\xi=r/a$ denotes the normalized radial coordinate; A_0 and B_0 are the constants given by $[2/wK_1(w)/K_0(w)+1]/(4u^2)$ and $[2/uJ_1(u)/J_0(u)-1]/(4w^2)$, respectively (these constants are obtained by matching tangential electric fields at the surface between the toroidal microcavity and the surrounding material); C_0, D_0, E_0, and F_0 are the constants similarly obtained; u and w are the normalized toroidal microcavity parameters ($u^2+w^2=v^2$ where v is the v parameter defined similarly for the case of weakly guiding fiber [20]), J_j denotes the Bessel function of the jth order, and K_j denotes the modified Hankel functions of the jth order. For higher-order transverse modes with $l \ge 1$, the cavity mode field can be obtained similarly. For quasi-TE modes, the magnetic field is then given by

$$\vec{H} = -\frac{1}{j\omega\mu}\vec{\nabla}\times\vec{E} \approx -\frac{1}{j\omega\mu}\vec{\nabla}\times(\hat{\phi}E_\phi). \tag{17}$$

After evaluating the above expression in the local toroidal coordinates, the tangential magnetic field is given by

$$H_\theta = -\frac{1}{j\omega\mu}\left[\frac{1}{r} + \frac{\partial}{\partial r}\right]E_\phi(r,\phi). \tag{18}$$

Matching H_θ at the toroidal microcavity surface $r=a$ gives the following characteristic equation for quasi-TE modes:

$$u\frac{J_1(u)}{J_0(u)} = w\frac{K_1(w)}{K_0(w)} \quad (\mathrm{TE}_{q0m}\ \mathrm{mode}), \tag{19}$$

where $u=a\sqrt{(nk)^2-\beta^2}$ and $w=a\sqrt{\beta^2-(n_0k)^2}$. Using this characteristic equation along with the quantization of the intrinsic propagation constant $\beta=m/R$, rough estimates of the resonance wavelengths and the FSR (free spectral range) can be obtained from Eq. (19). However, for a more precise prediction of the cavity mode field and the resonance wavelengths, an iterative modification of the intrinsic propagation constant and normalized toroidal microcavity parameters is required using the following modified characteristic equation:

$$u_e\frac{J_1(u_e)}{J_0(u_e)} = w_e\frac{K_1(w_e)}{K_0(w_e)} \quad (\mathrm{TE}_{q0m}\ \mathrm{mode}), \tag{20}$$

where $u_e=a\sqrt{(nk)^2-\beta_e^2}$, $w_e=a\sqrt{\beta_e^2-(n_0k)^2}$, and β_e is the modified propagation constant. For this purpose, an effective radial coordinate r_e and an effective radius R_e of the toroidal microcavity are defined as follows (for the case of small inverse aspect ratio):

$$r_e \equiv a\frac{\int\int \varepsilon|\vec{E}|^2\xi^2\cos\phi d\xi d\phi}{\int\int \varepsilon|\vec{E}|^2\xi d\xi d\phi}, \tag{21}$$

$$R_e = R + r_e = R\left(1 + \delta\frac{\int\int \varepsilon|\vec{E}|^2\xi^2\cos\phi d\xi d\phi}{\int\int \varepsilon|\vec{E}|^2\xi d\xi d\phi}\right). \quad (22)$$

The iteration procedure proceeds as follows. After obtaining the effective radius R_e with the intrinsic propagation constant β, the resonance wavelength (including the normalized toroidal microcavity parameters u and w) is updated with the modified propagation constant β_e and the modified characteristic equation (20). The modified propagation constant β_e can be obtained by projecting the intrinsic propagation constant β to the effective radius R_e [21] as follows:

$$\beta_e = \beta\left(1 + \frac{a_e}{2R}\right)^{-1} = 2\beta\left(1 + \frac{R_e}{R}\right)^{-1}. \quad (23)$$

After several iterations with Eqs. (20)–(23) and the field expressions (11)–(16), all the relevant parameters converge rapidly to the constant values, including the resonance wavelength (the convergence required two to four iterations for the examples given in this paper to give a relatively small error). Physically, the iteration procedure described here accounts for the mode pattern shift relative to the straight waveguide geometry.

Using the results of the iterative procedure, an asymptotic formula for the modified propagation constant β_e of the fundamental quasi-TE mode is found by applying a fitting procedure. With this empirical formula, the cavity mode field at the specified resonance wavelength can be directly obtained without resorting to the iterative procedure:

$$\beta_e \approx \frac{2\pi}{\lambda}\left\{n - (2-n)\left[1 + \zeta\left(\frac{a}{\lambda/n}\right)^2\right]^{-1}\right\}, \quad (24)$$

where $\zeta = 6.8288$ gives a very good estimate to the modified propagation constant β_e. With a test fitting in the wavelength bands of 850 and 1550 nm, the error was found to be below ~1% for the toroidal microcavity with principal diameter ranging from 40 to 80 μm. Figure 3 plots the effective mode index ($n_e = \beta_e/k$) of the fundamental quasi-TE mode as a function of minor radius using both the iterative procedure and Eq. (24). It is worthwhile to note that the principal diameter has a negligible effect on the evaluation of the modified propagation constant for the case of $R_p \gg \lambda$.

Figure 4 shows the normalized squared transverse electric field [fundamental quasi-TE mode with $(q,l) = (0,0)$] calculated from the iterative perturbation theory for a toroidal microcavity with minor (principal) diameters of 3 (60) μm along with a theoretical prediction provided by a FEM simulation. An excellent agreement between the numerical and the perturbative analytic evaluation can be confirmed. It can be seen that the peak of the cavity mode field shifts towards the toroid exterior due to the curvature of the geometrical boundary. As the radial mode number q increases, the amount of peak shift generally decreases compared to that of a fundamental mode and the number of squared cavity mode field maxima in the equatorial plane increases as $2q+1$ (see Fig. 5).

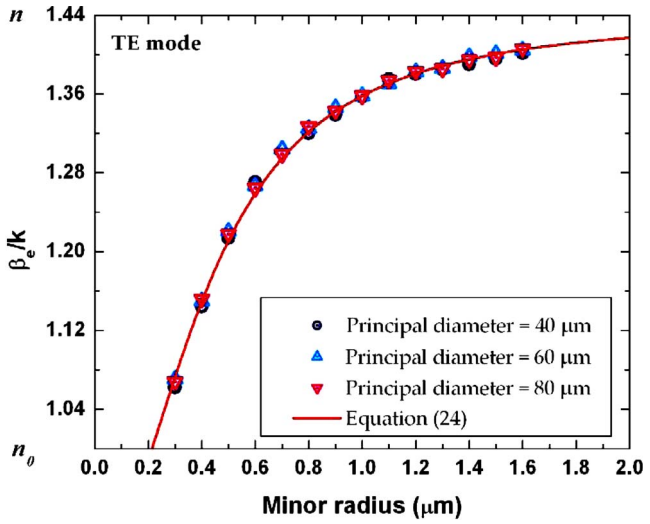

FIG. 3. (Color online) The mode index ($n_e = \beta_e/k$) of the fundamental quasi-TE mode as a function of minor radius. The iteration method gives a slight variation in the mode index due to the change in actual resonance wavelengths (~1550 nm) for different minor diameters.

Figure 6 shows the finite element simulation of the squared transverse electric fields of the quasi-TE/TM modes for a fixed azimuthal mode number $m = 163$. The supported modes for this specific cavity are shown with their mode numbers $(q,l) = (0,0)$, $(0,1)$, $(0,2)$, and $(1,0)$, respectively. In this case, the fundamental quasi-TE mode is located at 1548.79 nm and the higher-order modes are located at shorter wavelengths.

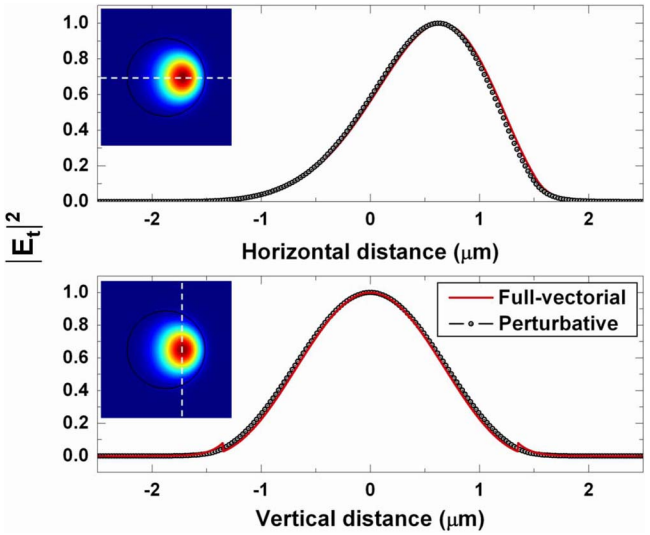

FIG. 4. (Color online) The normalized squared transverse electric field [fundamental quasi-TE mode with $(q,l) = (0,0)$] calculated from iterative perturbation theory for a toroidal microcavity with a minor (principal) diameter of 3 (60) μm along with a theoretical prediction provided by a finite element method (FEM) simulation.

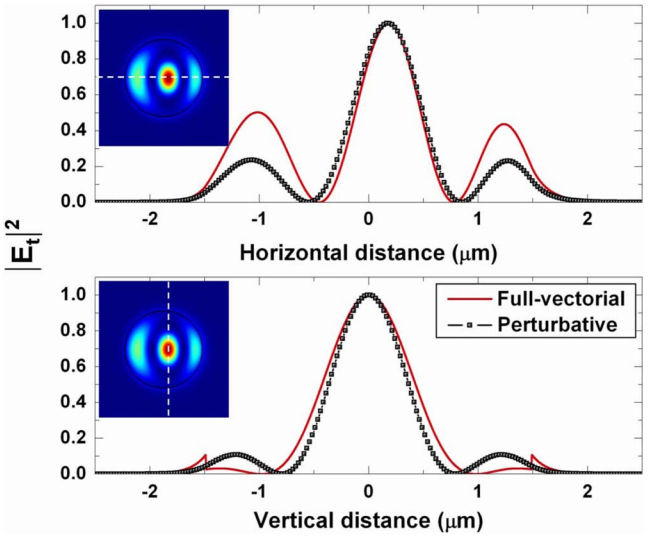

FIG. 5. (Color online) The normalized squared transverse electric field [quasi-TE mode with $(q,l)=(1,0)$] calculated from iterative perturbation theory along with a theoretical prediction provided by a finite element method (FEM) simulation.

Resonance wavelengths of toroidal microcavity

Resonance wavelengths of a toroidal microcavity and the corresponding FSRs can be obtained as described in the previous section for each quasi-TE/TM mode using the characteristic equation along with the iteratively obtained propagation constant β_e. (For the purpose of resonance wavelength prediction, eigenvalues of the characteristic equation are assumed to be real. However, it is worthwhile mentioning that the eigenvalues can be complex in general and the complex-valued eigenvalues will give a simple estimation of the radiative Q factor [22,23]. This issue will be studied in a later section.)

The dependency of wavelength shifts on lateral dimension can be intuitively understood by a simple analogy. After having separated the azimuthal θ dependence, the problem reduces to that of a two-dimensional potential well for the confined eigenmodes (effective potential depends on the difference in the refractive index and the curvature). As the dimension of the toroidal microcavity (minor diameter) decreases for a fixed principal diameter, the eigenfrequency spectrum (resonance wavelength) moves towards a higher-energy level (shorter wavelength). This resonance wavelength blue shift is more pronounced if the minor diameter of a toroidal microcavity becomes more compressed to a fiber-like geometry due to the presence of additional confinements from the radial direction.

Figure 7 shows the resonance wavelengths for two adjacent azimuthal mode numbers $m=157$ and 158 as a function of minor diameter (the principal diameter of the toroidal microcavity is fixed at 60 μm) [24]. An excellent agreement in resonance wavelengths is confirmed by comparison with FEM simulations. Also note that even though the iterative prediction for the resonance wavelength starts to deviate slightly as the minor diameter becomes larger, the FSR of the microcavity still remains accurate due to the error canceling as shown in Fig. 8.

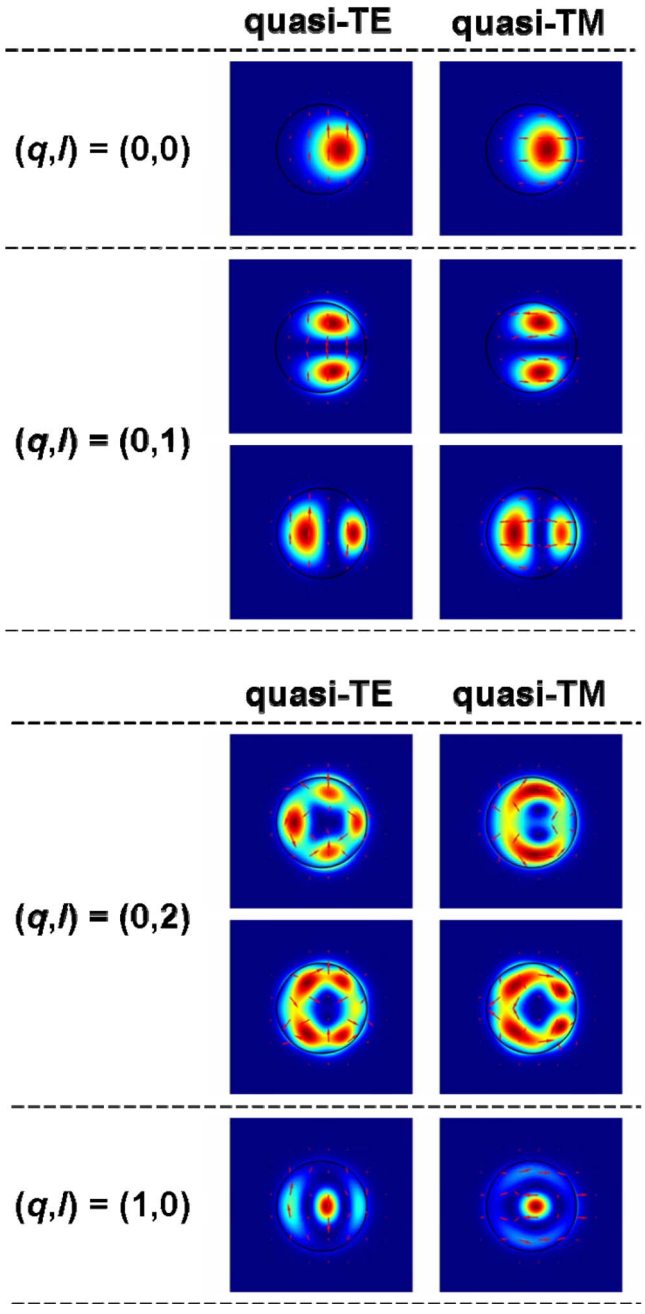

FIG. 6. (Color online) Squared transverse electric fields for a toroidal microcavity with a minor (principal) diameter of 3 (60) μm.

Mode volume of toroidal microcavity

The mode volume of a microcavity has a substantial impact on various experiments and theoretical predictions. On the assumption that the cavity quality factor can be maintained at the same level, smaller mode volume is generally preferred to larger mode volume in nonlinear optics, the Purcell effect, cavity quantum electrodynamics, and in lowering the lasing threshold of microcavity lasers. The mode volume of a toroidal microcavity can be engineered by independently modifying the major (minor) diameters (while for spherical resonators, only the diameter of the sphere can be con-

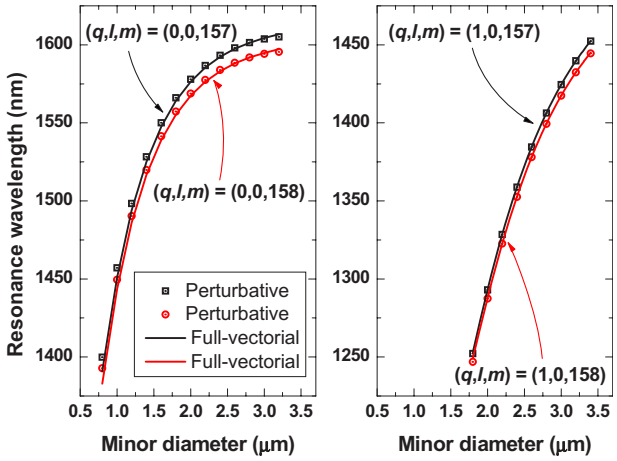

FIG. 7. (Color online) Left: resonance wavelengths for fundamental quasi-TE_{00m} modes as a function of a minor diameter (principal diameter of toroidal microcavity is fixed at 60 μm). Resonance wavelengths are plotted for two adjacent azimuthal mode numbers $m=157$ and 158. Right: resonance wavelengths for quasi-TE_{10m} modes.

trolled), or by changing the refractive index of the cavity material. With the cavity mode fields obtained using the perturbation analysis, the mode volume of a microcavity with small inverse aspect ratio can be calculated in the local toroidal coordinate system using the definition of the cavity mode volume as follows:

$$V = \frac{\int\int\int \varepsilon(\vec{r})|\vec{E}(\vec{r})|^2 d^3\vec{r}}{|\vec{E}(\vec{r})|^2_{\max}}. \tag{25}$$

The formula for the electric field given in Eq. (6) can be inserted into the above expression and evaluated numerically.

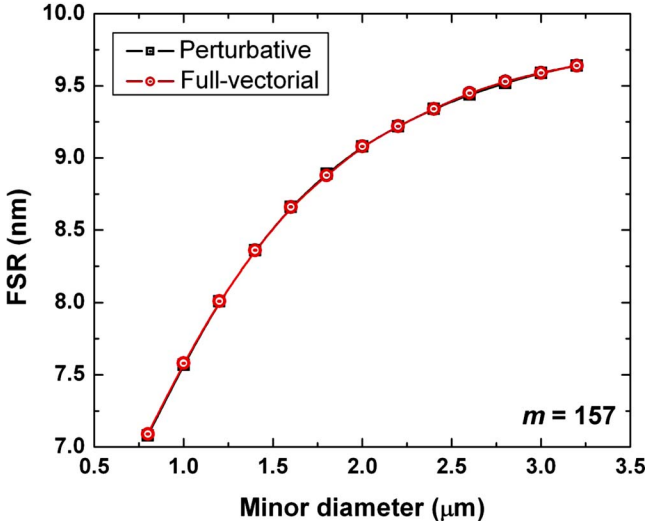

FIG. 8. (Color online) FSR calculated for the fundamental cavity mode $m=157$ and 158 as a function of the minor diameter (the principal diameter of the toroidal microcavity is fixed at 60 μm).

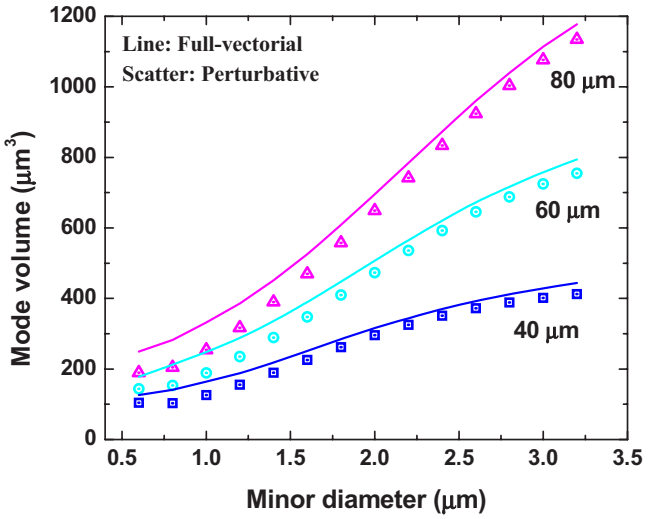

FIG. 9. (Color online) Calculated mode volume V of a fundamental $(q,l)=(0,0)$ mode of the toroidal microcavity for small inverse aspect ratio.

Figure 9 shows the calculated mode volume V of the fundamental $(q,l)=(0,0)$ mode of the toroidal microcavity for small inverse aspect ratio. The applicability of the iterative perturbation expansion is limited to the small inverse aspect ratio regime where the toroid is fiberlike. Deviations from predictions of mode volume based on a finite element analysis begin to appear as the aspect ratio is reduced. Figure 10 shows the mode volume of higher-order modes calculated using both the perturbative analytic theory and a finite element solver. For a fixed aspect ratio, it is found that higher-order modes can have a smaller-mode volume mode than the fundamental mode. However, the fundamental mode has a global minimum in the mode volume.

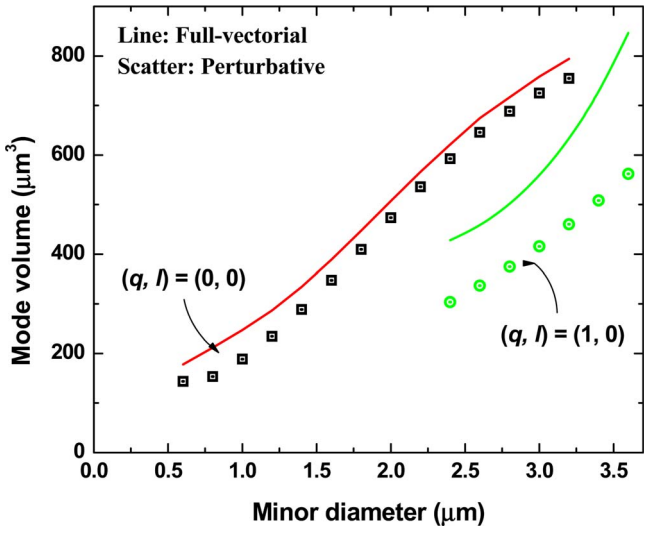

FIG. 10. (Color online) Mode volume of higher-order modes calculated using the finite element method and the perturbative analytic calculations (the principal diameter of the toroidal microcavity is fixed at 60 μm).

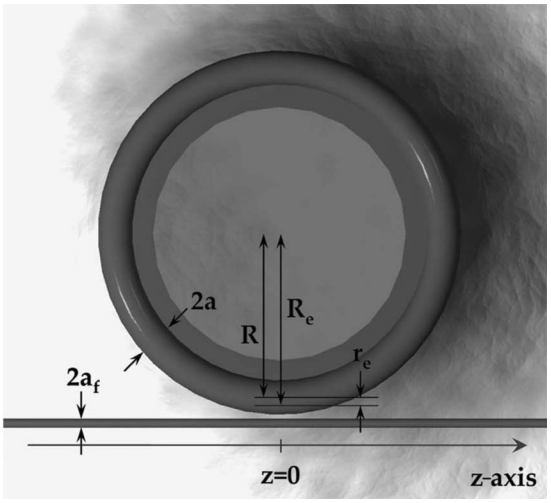

FIG. 11. Geometry and parameters of toroidal microcavity and tapered fiber used to derive the phase-matching condition.

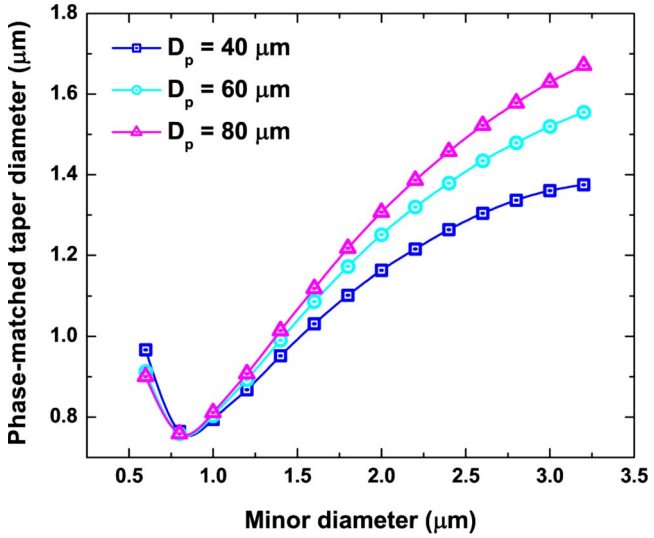

FIG. 12. (Color online) Phase-matched tapered fiber diameter as a function of the minor diameter for toroidal microcavities with 40, 60, and 80 μm principal diameter.

Phase-matching Conditions

Phase matching between the cavity mode and the waveguide mode is a necessary condition that permits the coupling of waves into and out of microcavity resonators. To access all three regimes of coupling (undercoupled, overcoupled, and critically coupled regime) with a variation in gap width between the waveguide and the microcavity, some control of the phase-matching condition is essential (in addition to a high enough intrinsic cavity Q factor). The simple phase-matching criterion can be written as

$$\beta_e = \beta_{taper}. \tag{26}$$

Phase mismatch (i.e., the difference in propagation constants $\Delta\beta$), however, is present even for the toroidal microcavity and the tapered fiber with the same propagation constants and this is caused by the curved geometry of the cavity. To transform the propagation constant β_e in the curved geometry into the equivalent propagation constant $\beta_{e,tr}$ in straight waveguide coordinates (as seen by the straight tapered fiber), the following mapping formula can be used [21]:

$$\beta_{e,tr} \approx \left[1 - \frac{d_{sep}}{2R_e} - \left(\frac{z}{2R_e}\right)^2\right]\beta_e, \tag{27}$$

where β_e is the modified propagation constant obtained by the iterative method. At the minimum separation between the toroidal microcavity and the tapered fiber, i.e., $z=0$, the effective propagation constant projected onto the axis of a straight tapered fiber can be written (assuming $d_{sep} = a - r_e + a_f$, where a_f denotes the tapered fiber radius, see Fig. 11) as follows:

$$\beta_{e,tr}(z=0) \approx \left[1 - \left(\frac{a - r_e + a_f}{2R_e}\right)\right]\beta_e. \tag{28}$$

The propagation constant β_{taper} of the tapered fiber mode HE_{11} can be solved as a function of the tapered fiber radius a_f using the following characteristic equation [25]:

$$\frac{J_0(u_f)}{u_f J_1(u_f)} = -\left(\frac{n_f^2 + n_0^2}{2n_f^2}\right)\frac{K_1'(w_f)}{w_f K_1(w_f)} + \left(\frac{1}{u_f^2} - R\right), \tag{29}$$

where

$$R = \left[\left(\frac{n_f^2 - n_0^2}{2n_f^2}\right)^2\left(\frac{K_1'(w_f)}{w_f K_1(w_f)}\right)^2 + \left(\frac{\beta_{taper}}{n_f k}\right)^2\left(\frac{1}{w_f^2} + \frac{1}{u_f^2}\right)^2\right]^{1/2},$$

$$u_f = a_f\sqrt{(n_f k)^2 - \beta_{taper}^2}, \quad w_f = a_f\sqrt{\beta_{taper}^2 - (n_0 k)^2},$$

where n_f denotes the refractive index of the tapered fiber and n_0 is the refractive index of the surrounding. The following transcendental equation should then be solved for a phase-matched diameter of the tapered fiber:

$$\beta_{taper}(a_f) \approx \left[1 - \left(\frac{a - r_e + a_f}{2R_e}\right)\right]\beta_e(a). \tag{30}$$

Figure 12 shows the phase-matched tapered waveguide diameter as a function of the minor diameter for fixed toroidal microcavity principal diameters of 40, 60, and 80 μm. For a very small minor diameter ($d < 0.8$ μm), the phase-matched tapered waveguide diameter decreases as the minor diameter of the toroidal microcavity becomes larger. In this regime, the decrease of the phase-matched diameter is mainly caused by the decrease of the effective radial coordinate r_e. For a slightly larger minor diameters, the phase-matched tapered fiber diameter increases as the minor diameter becomes larger. This increase of phase-matched diameter slows due to the slow increase of β_e for larger minor diameters. In addition, it can be clearly seen that the phase-matched fiber diameter increases for larger principal diameter toroidal microcavity for a fixed minor diameter. However, it should be noted that, for a larger tapered fiber diameter, higher-order tapered fiber modes can be present and the ideality of the coupled cavity-taper system can be degraded [26].

Whispering gallery loss of the toroidal microcavity

The loss of a surface-tension-induced optical cavity consists of several contributions. Among these, the whispering-gallery loss (or the radiative loss), which is induced by the curvature of the dielectric cavity, can be a dominating factor especially for small toroidal microcavities. As an aside, note that for a spherical microcavity, the only dimension of interest is the diameter. However, the situation is slightly different for a toroidal microcavity where additional compressions in the polar or radial direction increase radiative loss when compared to the spherical microcavity, especially for small inverse aspect ratio δ. In this section, the radiation loss of toroidal microcavity resonators will be computed using the "volume current method" (VCM). In this approach, the polarization current density created by the electric field inside the dielectric microcavity [given by $\vec{J}(r,\phi,\theta)=\varepsilon_0\omega\Delta\varepsilon\vec{E}(r,\phi,\theta)$] acts as a polarization current source, and this induces a far field (vector potential $\vec{A}$) by a scalar Green's function. By calculating the Poynting vector $\vec{S}$ from this vector potential, the radiation loss (i.e., whispering gallery loss) can be calculated. A similar problem, the radiation loss calculation of a bent optical fiber, has been studied in many papers [27,28]. One of these, an approach given by Kuznetsov and Haus [28], can be modified to fit our current toroidal microcavity geometry. The same approach has also been shown to be applicable to the case of microsphere resonators [27]. Using this method, the radiative Q factor of a toroidal microcavity can be formulated as [29]

$$Q_{rad} \approx \frac{\pi n^2 R_e}{\lambda Z_0 \int S_{r'} r'^2 \sin\theta' d\theta'}, \tag{31}$$

where Z_0 denotes the impedance of free space ($Z_0 \approx 377$) and $S_{r'}$ is the magnitude of the Poynting vector in the radial direction of the spherical polar coordinates used to describe the far field (primes are used for the spherical polar coordinates). Figure 13 shows the calculated radiative Q factor for fundamental quasi-TE modes as a function of the minor diameter of toroidal microcavities with principal diameters of 40, 60, and 80 μm. The resonance wavelengths were chosen to be located near 1550 nm. As can be confirmed from Fig. 13, the whispering-gallery loss is a sensitive function of the minor diameter. As the size of minor diameter decreases, the radiative Q factor decreases very quickly in the regime of small inverse aspect ratio due to the additional leakage of confined modes, which is induced by the increased compression in the toroidal boundary.

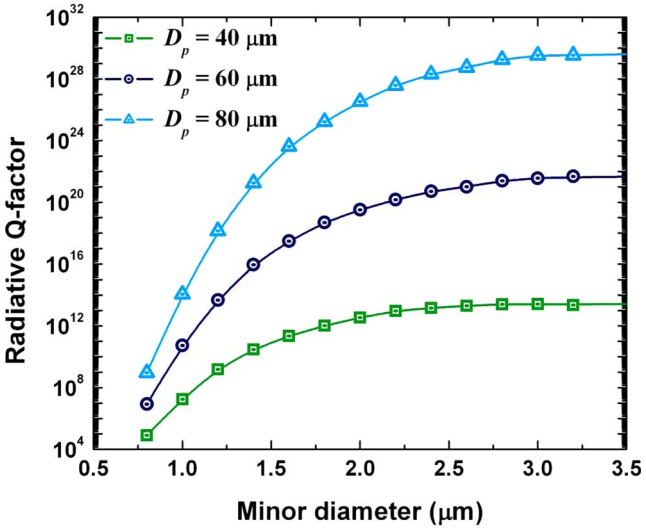

FIG. 13. (Color online) Radiative Q- factor for fundamental quasi-TE modes of toroidal microcavities with principal diameters of 40, 60, and 80 μm. The resonance wavelengths were chosen to be near 1550 nm.

CONCLUSIONS

A perturbative analytic method utilizing a perturbation expansion combined with an iterative procedure have been demonstrated and used to provide predictions for eigenfrequencies, mode volumes, phase-matching conditions, and radiative Q factor in microtoidal resonators. The expansion method relies upon the similarity between optical fiber waveguides and toroidal resonators and uses an expansion parameter based upon the inverse of the toroidal aspect ratio. The analysis method is in excellent agreement with the predictions of a finite element simulation and promises a simplification of analysis of toroidal microcavities in the important, high-aspect-ratio regime.

ACKNOWLEDGMENTS

This work was supported by DARPA, NSF, Caltech Lee Center, and the plasmonic MURI.

[1] D. K. Armani, T. J. Kippenberg, S. M. Spillane, and K. J. Vahala, Nature (London) **421**, 925 (2003).
[2] M. L. Gorodetsky, A. A. Savchenkov, and V. S. Ilchenko, Opt. Lett. **21**, 453 (1996).
[3] D. Armani, B. Min, A. Martin, and K. J. Vahala, Appl. Phys. Lett. **85**, 5439 (2004).
[4] T. J. Kippenberg, S. M. Spillane, D. K. Armani, and K. J. Vahala, Opt. Lett. **29**, 1224 (2004).
[5] L. Yang, T. Carmon, B. Min, S. M. Spillane, and K. J. Vahala, Appl. Phys. Lett. **86**, 091114 (2005).
[6] B. Min, T. J. Kippenberg, L. Yang, K. J. Vahala, J. Kalkman, and A. Polman, Phys. Rev. A **70**, 033803 (2004).
[7] T. J. Kippenberg, S. M. Spillane, and K. J. Vahala, Phys. Rev. Lett. **93**, 083904 (2004).
[8] B. Min, L. Yang, and K. J. Vahala, Appl. Phys. Lett. **87**, 181109 (2005).

[9] S. M. Spillane, T. J. Kippenberg, K. J. Vahala, K. W. Goh, E. Wilcut, and H. J. Kimble, Phys. Rev. A **71**, 013817 (2005).
[10] T. Aoki, B. Dayan, E. Wilcut, W. P. Bowen, A. S. Parkins, T. J. Kippenberg, K. J. Vahala, and H. J. Kimble, Nature (London) **443**, 671 (2006).
[11] A. M. Armani and K. J. Vahala, Opt. Lett. **31**, 1896 (2006).
[12] A. M. Armani, D. K. Armani, B. Min, K. J. Vahala, and S. M. Spillane, Appl. Phys. Lett. **87**, 151118 (2005).
[13] S. J. Garth, IEE Proc.-J: Optoelectron. **134**, 221 (1987).
[14] F. L. Teixeira and W. C. Chew, IEEE Microw. Guid. Wave Lett. **7**, 371 (1997).
[15] B. Lamouroux, B. Prade, and J. Y. Vinet, J. Mod. Opt. **38**, 761 (1991).
[16] B. E. Little, J.-P. Laine, and H. A. Haus, J. Lightwave Technol. **17**, 704 (1999).
[17] For the simplicity of satisfying the boundary condition, the polarization direction is assumed to be in the ϕ direction rather than in the z direction. This approximation breaks down for a toroidal microcavity with very small inverse aspect ratio.
[18] For real toroidal microcavities, the toroidal part is always attached to a silica supporting disk and a silicon pillar. This, however, has secondary effects on the cavity mode fields and this effect is more prominent for the case of small inverse aspect ratio for a fixed disk dimension. Qualitatively speaking, the radiative Q factor drops and the mode volume increases when compared to the ideal case without the supporting disk. The change in the Q factor, mode volume, and resonance wavelength is varied for different modes. Generally, higher-order modes are more sensitive to the supporting disk structure than the fundamental modes. However, in this paper, the effect of the supporting disk is not considered for a consistent analysis.
[19] In the original paper written for a bent optical fiber [13], the propagation constant β is also expanded as $\beta^2=\beta_0^2+\beta_2^2\delta^2$. However, this makes the cavity field expression more complicated when the desired order of perturbation theory becomes larger. Therefore, in this chapter, a different approach has been taken to modify the propagation constant with the iterative method.
[20] D. Gloge, Appl. Opt. **10**, 2252 (1971).
[21] D. R. Rowland and J. D. Love, IEE Proc.-J: Optoelectron. **140**, 177 (1993).
[22] L. A. Weinstein, *Open Resonators and Open Waveguides* (The Golem Press, Boulder, Colorado, 1969), Chap. 9.
[23] A. N. Oraevsky, Quantum Electron. **32**, 377 (2002).
[24] The number of modes supported by the toroidal microcavity strongly depends on the size of the cavity. Especially, the minor diameter of the toroidal microcavity has a direct impact on the number of supported modes. Therefore, when compared to the microsphere resonators, the mode spectra in the transmission measurement are greatly simplified due to the decreased number of supported modes for a toroidal microcavity and especially for a toroid with a small inverse aspect ratio.
[25] A. Yariv, *Optical Electronics in Modern Communications* (Oxford University Press, New York, 1997), Chap. 3.
[26] S. M. Spillane, T. J. Kippenberg, O. J. Painter, and K. J. Vahala, Phys. Rev. Lett. **91**, 043902 (2003).
[27] A. W. Snyder, I. White, and D. J. Mitchell, Electron. Lett. **11**, 332 (1975).
[28] M. Kuznetsov and H. A. Haus, IEEE J. Quantum Electron. **QE-19**, 1505 (1983).
[29] In this approximation, electric field polarization is assumed to be normal to the equatorial plane. This approximation is intuitively justified especially for the fundamental mode, which has a higher field density concentrated near the equatorial plane, $\phi \ll 1$.